applied optics

Suppression of FM-to-AM modulation by polarizing fiber front end for high-power lasers

Zhi Qiao,[1,2] Xiaochao Wang,[1] Wei Fan,[1,*] Xuechun Li,[1] Youen Jiang,[1] Rao Li,[1,2] Canhong Huang,[1,2] and Zunqi Lin[1]

[1]National Laboratory on High Power Lasers and Physics, Shanghai Institute of Optics and Fine Mechanics, Chinese Academy of Science, Shanghai 201800, China
[2]University of the Chinese Academy of Sciences, Beijing 100049, China
*Corresponding author: fanweil@siom.ac.cn

Received 30 June 2016; revised 1 September 2016; accepted 11 September 2016; posted 12 September 2016 (Doc. ID 269332); published 10 October 2016

FM-to-AM modulation is an important effect in the front end of high-power lasers that influences the temporal profile. Various methods have been implemented in standard-fiber and polarization-maintaining (PM)-fiber front ends to suppress the FM-to-AM modulation. To analyze the modulation in the front end, a theoretical model is established and detailed simulations carried out that show that the polarizing (PZ) fiber, whose fast axis has a large loss, can successfully suppress the modulation. Moreover, the stability of the FM-to-AM modulation can be improved, which is important for the front end to obtain a stable output. To verify the model, a PZ fiber front end is constructed experimentally. The FM-to-AM modulation, without any compensation, is less than 4%, whereas that of the PM fiber front end with the same structure is nearly 20%. The stability of the FM-to-AM modulation depth is analyzed experimentally and the peak-to-peak and standard deviation (SD) are 2% and 0.38%, respectively, over 3 h. The experimental results agree with the simulation results and both prove that the PZ fiber front end can successfully suppress the FM-to-AM conversion. The PZ fiber front end is a promising alternative for improving the performance of the front end in high-power laser facilities. © 2016 Optical Society of America

OCIS codes: (140.3518) Lasers, frequency modulated; (060.5060) Phase modulation; (070.7345) Wave propagation; (350.2660) Fusion.

http://dx.doi.org/10.1364/AO.55.008352

1. INTRODUCTION

Since the first Ruby laser was invented, high-power or high-energy lasers have been an interesting field that attracts considerable of attention. High-power or high-energy lasers are excellent tools for investigating high-density physics, high-intensity interactions between light and matter, and plasma physics. Especially for the inertial confinement fusion (ICF), high-energy lasers are crucial for achieving laser fusion where the target is compressed by high-energy nanosecond lasers for the direct-driven fusion, or by x rays generated by the interaction between high-energy lasers and a hohlraum for the indirect-driven fusion [1,2]. Because of the complex time-dependent interaction process between laser pulses and plasma, high-energy lasers must be precisely shaped to achieve optimal performance. For a high-energy laser facility, stimulated Brillouin scattering (SBS) should be avoided; otherwise, expensive large-aperture optical elements can be permanently damaged. The threshold of SBS is directly linked to the bandwidth of laser pulses, so that the spectrum broadening of high-energy lasers is an efficient method for interrupting the growth of the SBS laser [3,4]. In addition to the requirement to suppress SBS, the smoothing of spectral dispersing (SSD) also needs the high-energy laser to be temporally phase-modulated [5]. The uniform laser spot is desired both in direct and indirect laser fusion processes, where a slight nonuniformity will cause instability of the laser compression. SSD is an effective technique for obtaining time-averaged smooth illumination. For a large laser facility, the phase-modulation technique, which can temporally modulate the laser pulse to generate multiple spectral sidebands, is applied in the front end. In addition to the spectral broadening, the front end supplies a temporally synchronized, precisely shaped, stable, and clean seed laser for the whole high-energy laser system. Although the phase-modulation process gives contribution to the SSD and suppression of SBS, the FM-to-AM conversion, which affects the laser temporal profile, occurs in high-energy lasers such as National Ignition Facility, the Laser Mégajoule Facility, and the ShengGuang series [6–8]. The FM-to-AM conversion can be induced by the nonuniform spectral transmission and dispersion. The nonuniform spectral transmission

in a facility can be precompensated easily by elements with a proper contrary spectral transmission [9–11]. However, the FM-to-AM conversion induced by dispersion, which includes group velocity dispersion (GVD) and polarization mode dispersion (PMD) is complex. The GVD of the whole system can be simply precompensated by a pair of gratings or prisms, whereas the PMD is far more complicated. Ordinarily, the front end is consisted of either standard single-mode (SM) fiber elements or polarization maintaining (PM) fiber elements. The front end based on the PM fiber is more stable than the SM fiber structure; therefore the PM fiber is a prior choice for high-energy laser systems. Nevertheless, the PMD in PM fiber is difficult to control, and various methods have been proposed for suppressing the FM-to-AM conversion in a polarization-maintained front end [12,13]. The PM fiber is sensitive to environmental conditions, which induces a recombination phase which varies randomly in the PM fiber. The temperature, pressure, and bending affect the recombination phase, such that the FM-to-AM conversion differs temporally and randomly. The uncertainty of the FM-to-AM modulation increases the risk of damage to optical elements due to the extraordinarily high peak power of laser pulses.

In addition to the PM fiber, the PZ fiber can also preserve the polarization of laser pulses [14–16]. In contrast to the PM fiber, the laser transmitting along the fast axis experiences a large loss; therefore, the effect of the PMD can be minimized. This advantage makes the PZ fiber suitable for the front end of high-energy lasers [17]. To suppress the FM-to-AM conversion, we proposed a front end consisting of all polarizing fiber elements for the first time to the best of our knowledge, while the traditional front ends are consisted with either standard single-mode fiber or polarization maintaining fiber. It is found that the PZ fiber front end has advantages in the suppression of FM-to-AM modulation, stability and the complexity compared with the PM or SM fiber front end. The front end was analyzed theoretically and experimentally and the experimental results show that the FM-to-AM modulation was successfully suppressed. In Section 2, the propagation of a laser in the PZ fiber front end is analyzed theoretically, and a model for calculating the FM-to-AM conversion is proposed. Section 3 presents the detailed simulation of the FM-to-AM conversion in the PZ fiber front end and the difference is discussed with respect to the PM fiber front end. The experimental results for the PZ fiber front end are discussed in Section 4. The FM-to-AM modulation of the PZ fiber front end system is negligible, and the limitation of the FM-to-AM conversion comes from the GVD in the PZ fiber, which can be easily compensated for. Additional discussions and conclusions are presented in Section 5.

2. SIGNAL PROPAGATION IN FRONT END SYSTEM

The propagation of the laser pulse in the polarization-maintaining or polarizing fiber can be described as shown in Fig. 1. The laser pulse is injected into the fiber patch with an angle θ_{in}, which is the angle between the polarization of the laser and the slow axis of the fiber patch. During the propagation in the fiber, the group velocity dispersion (GVD) and

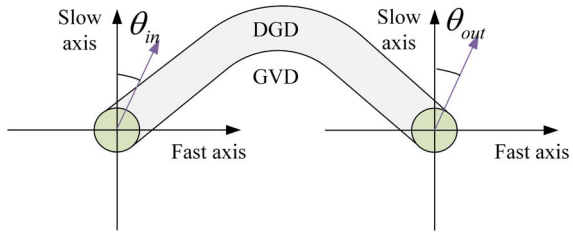

Fig. 1. Illustration of pulse propagation in a polarization-maintaining or polarizing fiber.

differential group delay (DGD) are the two main factors affecting the laser. In addition to the GVD and DGD, the natural polarization-mode mixing effect, which is related to the polarization extinction ratio (PER), of the PM or PZ fiber should also be considered. When the laser is transmitted outside the fiber patch, its polarization has an angle θ_{out} with the slow axis of the fiber. The propagation process shown in Fig. 1 can be modeled by the Jones transfer matrix. The laser after the fiber patch is given in the frequency domain as

$$\tilde{E}_{\text{out}} = C_{\text{out}} P_f C_{\text{in}} \tilde{E}_{\text{in}}, \tag{1}$$

where C_{in} and C_{out} are the rotation of the laser relative to the slow axis of the fiber, and can be expressed as

$$C_{\text{in,out}} = \begin{pmatrix} \cos(\theta_{\text{in,out}}) & -\sin(\theta_{\text{in,out}}) \\ \sin(\theta_{\text{in,out}}) & \cos(\theta_{\text{in,out}}) \end{pmatrix}. \tag{2}$$

$\tilde{E}_{\text{in}}$ is the laser transmitted into the fiber, and can be written as

$$\tilde{E}_{\text{in}} = \begin{pmatrix} \tilde{E}_{\text{in}}^{\text{slow}} \\ \tilde{E}_{\text{in}}^{\text{fast}} \end{pmatrix}. \tag{3}$$

The PER is included in P_f in the Eq. (1) and is given as

$$P_f = G_p \begin{pmatrix} \cos(\theta_p) & -\sin(\theta_p) \\ \sin(\theta_p) & \cos(\theta_p) \end{pmatrix} G_P, \tag{4}$$

where θ_p is related to the PER of fiber as follows [16]:

$$\theta_p = \arctan\left(\sqrt{1/\text{PER}}\right). \tag{5}$$

The GVD and DGD have a great influence on the FM-to-AM conversion, and the two effects are considered in G_p, which can be written as

$$G_P = e^{i\beta_2 L\omega^2/4} \begin{pmatrix} e^{-\alpha_{\text{slow}} L/4} & 0 \\ 0 & e^{-\alpha_{\text{fast}} L/4 - i\epsilon\omega L/2 - i\varphi_p} \end{pmatrix}, \tag{6}$$

where L is the fiber length; ϵ denotes the DGD coefficient, which is normally between 1.5 and 2 ps/m in a polarization-maintaining fiber; φ_p is a part of the DGD in PM fibers and fluctuates randomly with environmental conditions, such as the stress and temperature; and α_{slow} and α_{fast} are the losses occurring when the laser is transmitted along the slow axis and fast axis, respectively, in the fiber. For the PM fiber, the losses for the slow axis and fast axis are the same and negligible. However, the loss for the fast axis in a polarizing fiber is significantly larger than that for the slow axis; thus, the fiber acts as a distributed polarizing element. To obtain a better accuracy, the fiber patch with a length of L is divided into two

segments between which the effect of the PER is considered, as shown in Eq. (4).

The propagation in a fiber patch can be modeled by Eq. (1) and is the basic process for modeling the front end. The front end is complex and comprises acoustic modulators, electro-optic modulators, phase modulators, fiber connectors, fiber splitters, fiber amplifiers, and numerous fiber patches. For simplicity, all of the components are decomposed into three basic parts: connections, fiber patches, and the inner-crystal part. There are three types of connections: fiber connectors, alignment connectors, and splices between fibers. Besides the modulators and fiber patches, there are a lot of other fiber components in the front end, such as fiber isolators, fiber bandpass filters, and fiber inline polarizers. These components have spatial parts, faraday rotators, filters, and polarizers, between the two segments of the fiber tail. Considering that the alignment accuracy of the two fiber segments affects the FM-to-AM conversion, this part is included in the connections as alignment connectors. The PER of fiber connectors is less than that of the splice and similar to that in Eq. (1), and the effect of connections is taken into account as

$$C_c = \begin{pmatrix} \cos(\theta_c) & -\sin(\theta_c) \\ \sin(\theta_c) & \cos(\theta_c) \end{pmatrix}, \tag{7}$$

where C_c is the rotation effect of connections, and θ_c is given by the PER of fiber connectors, alignment connectors, or fiber splices, as shown in Eq. (5). Fiber patches are calculated using Eq. (1), except that the rotation effect is given in the connections part. The inner-crystal part is quite different from the connections or fiber patches, and indicates the effect of the crystal inside the modulator, such as acoustic-optic crystals and electro-optic crystals. Usually, the crystal inside the modulators is a uniaxial crystal of which the birefringence must be considered. The Jones matrix of propagation in the inner-crystal part is given as

$$B = \begin{pmatrix} 1 & 0 \\ 0 & \eta \end{pmatrix} \begin{pmatrix} 1 & 0 \\ 0 & \exp(-i\tau_c\omega) \end{pmatrix}, \tag{8}$$

where η is the polarization loss if there is a polarizing part in the modulator, as there is for the electro-optic modulators, and is related to the PER of the polarizing component; and τ_c is the delay time between the ordinary and extraordinary light caused by the birefringence of the crystal. In addition to the birefringence, the alignment accuracy of the input fiber and output fiber with the crystal should be included as alignment connectors, as shown in Eq. (7).

Here, a simple example is provided to show how to calculate the propagation in the front end. Assuming that a fiber patch of 1 m is connected to a modulator that has 1 m input and output fibers with a fiber connector, and that after the modulator, a fiber isolator with 1 m input and output fiber is connected to a fiber splice, the propagation process can be written as

$$\tilde{E}_{\text{out}} = P_f C_a P_f C_s P_f C_a B C_a P_f C_c P_f \tilde{E}_{\text{in}}, \tag{9}$$

where C_a denotes the alignment connector, C_c denotes the fiber connector, C_s denotes the fiber splice, P_f denotes the fiber patch, and B denotes the birefringence of the crystal in the modulator. The Jones matrices shown in Eqs. (4), (7), and (8) provide the fundamental parts to model the whole front end, and detailed simulations are shown below.

3. SIMULATION OF FM-AM MODULATION

The basic structure of the front end for simulation is shown in Fig. 2, where the gray square denotes fiber connectors and the white cross denotes fiber splices. As shown in Fig. 2(a), the front end mainly consists of a continuum single-frequency laser (DFB), an acoustic-optic modulator (AOM), two fiber amplifiers (FA), a phase modulator (PM), and an electro-optic modulator (EOM). As previously mentioned, the modulators including the AOM, PM, and EOM can be simulated as two fiber segments and a birefringent crystal. The detailed structure of the fiber amplifier is shown in Fig. 2(b), and fiber components are connected by fiber splices. Considering the basic structure shown in Fig. 2(a), the front end can be modeled according the aforementioned theoretical analysis. The difference between the polarization-maintaining fiber and the polarizing fiber front ends is discussed, and the detailed simulations show that the polarizing fiber front end is more advantageous.

As shown in Fig. 2(a), the red line between the fiber connectors (gray square) is the fiber patch, which is 1 m in length. The modulators and fiber components, such as the ISO, WDM, IBP, and OC, have a fiber pigtail of 0.5 m. Except that the Yb-doped gain fiber is polarization-maintaining fiber due to the difficulty of manufacturing the polarizing gain fiber, all of the other components and fiber patches are made of either the PM fiber or PZ fiber. In the simulation, the PER of the PM fiber is 50 dB, with α_{slow} and α_{fast} equal to zero. The PER of the polarizing fiber is also 50 dB, but the fast axis of the polarizing fiber has a large loss, whereas the slow axis has a small loss owing to the special design. In the simulation, the losses of the slow and fast axis are zero and 15 dB/m, respectively. The delay time ϵ caused by the PMD is 1.6 ps/m for the PM and PZ fibers. The PER of the fiber components in the front end is the key factor which influences the FM-to-AM conversion, and cautious efforts must be made to guarantee the quality of fiber connectors and fiber splices. The PER of the fiber connectors is 22 dB, which is almost the highest that can be obtained. Compared with the fiber connectors, fiber splices are complex; the PER of splices of the standard PM fiber, which is the PANDA type, is 40 dB, while the PER of splices of the PZ

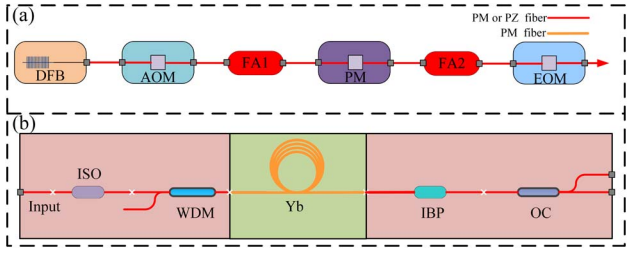

Fig. 2. Structure of the front end for FM-to-AM simulation. (a) Structure of the front end; (b) structure of the fiber amplifier. (DFB, distributed feedback CW laser; AOM, acoustic-optic modulator; FA1, FA2, fiber amplifiers; PM, phase modulator; EOM, electro-optic modulator; ISO, fiber isolator; WDM, wavelength division multiplex; Yb, Yb-doped fiber; IBP, fiber isolator and bandpass filter; OC, fiber coupler.)

fiber or PM fiber to PZ fiber, which is the bow-tie type, can only be 30 dB.

The fiber components, such as the ISO, WDM, IBP, and OC, consist of two fiber segments and one spatial element so that they can be modeled similarly to the modulator. Usually, the PER between the two fiber segments in the fiber components is 30 dB, and the effect of the fiber components can be regarded as a rotation in Eq. (7) together with two fiber pigtails. In contrast to the fiber components, the modulators contain birefringent crystals whose birefringence must be taken into account. The PER of the AOM is normally 25 dB, and the refraction ratios of ordinary and extraordinary light are 2.258 and 2.411, respectively, for a 10 mm TeO_2 crystal. The phase modulator is a $LiNbO_3$ waveguide phase modulator, and the commercial phase modulator is z-cut, which means that the polarization of the laser is along the z axis of the crystal. Therefore, the birefringence is not negligible, and the refraction ratios of ordinary and extraordinary light are 2.286 and 2.200, respectively, for the 30 mm $LiNbO_3$ crystal. The electro-optic modulator is also made of a $LiNbO_3$ crystal, but the polarization of the laser is along the x axis of the uniaxial crystal, so that the birefringence can be ignored. Using the Eqs. (1)–(8) and the parameters mentioned above, the FM-to-AM modulation can be analyzed theoretically. It should also be mentioned that the PERs of every element in the front end fluctuates in a range with a nearly normal distribution in the reality. Therefore, the mean values of the angles or PERs of various components in the front end are implemented to characterize the FM-to-AM modulation in the simulation for simplicity.

The FM-to-AM modulation is related to the laser spectrum, which is determined by the modulation depth and modulation frequency of the phase modulator in the front end. In the simulation, the modulation frequencies of the phase modulator are 3 GHz and 22 GHz, for which modulation depths are 0.25 and 0.95, respectively. The FM-to-AM modulation is characterized by the FM-to-AM modulation depth, which is defined as

$$\delta = 2\frac{I_{\max} - I_{\min}}{I_{\max} + I_{\min}}, \tag{10}$$

where $I_{\max}$ and $I_{\min}$ are the maximum and minimum of the fluctuation caused by FM-to-AM modulation, respectively.

The FM-to-AM conversion in the polarizing fiber front end is shown in Fig. 3. After the phase-modulation process, the spectrum of the laser pulse is broadened to 0.3 nm, as shown in Fig. 3(a), where the sideband of 22 and 3 GHz is obvious.

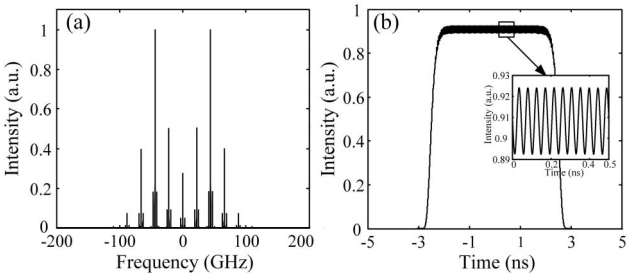

Fig. 3. Simulation of the polarizing fiber front end. (a) Spectrum of the laser after phase modulation, (b) laser pulse with FM-to-AM modulation in the polarizing fiber front end.

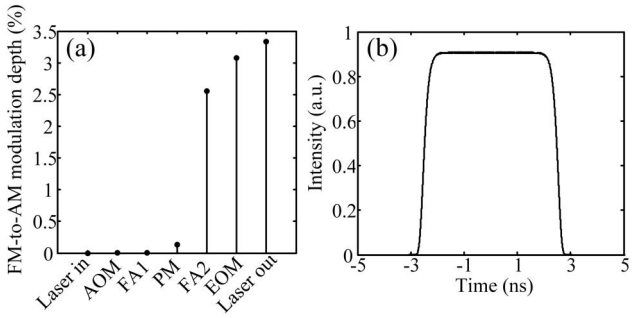

Fig. 4. FM-to-AM modulation in the polarizing fiber front end. (a) FM-to-AM modulation distribution at different positions, (b) laser after dispersion compensation.

Once the laser spectrum is broadened, the FM-to-AM modulation is obvious after the propagation in a series of components. The inserted figure in Fig. 3(b) is the magnified part of the waveform, which shows that the FM-to-AM modulation is 3.5%, corresponding to the 3 and 22 GHz phase modulation frequencies.

To investigate the FM-to-AM modulation in detail, the FM-to-AM modulation after each main component is shown in Fig. 4(a). The FM-to-AM modulation is zero before the phase modulator, as shown in Fig. 4(a), which is reasonable because the FM-to-AM conversion is actually the time-frequency transfer process. After the phase modulator, the spectrum is broadened so that the FM-to-AM modulation becomes obvious. The second PZ fiber amplifier induces more than 2% modulation because the total fiber length in the fiber amplifier is 7.5 m and the FM-to-AM modulation increases gradually due to the GVD of the PZ fiber. To verify whether the GVD is the main cause of the FM-to-AM modulation, the second-order dispersion compensation process is performed. The laser after dispersion compensation is shown in Fig. 4(b). After the dispersion compensation, the FM-to-AM modulation is 0.43%, which can be ignored. This result shows that the effect of the PMD is well eliminated and that if the GVD is compensated for, an excellent laser waveform can be obtained. The second-order dispersion can be easily compensated for by a pair of gratings, which makes the polarizing fiber front end suitable for generating high-quality shaped laser pulses.

The PM fiber front end is also analyzed to compare with the polarizing fiber system, and results are shown in Fig. 5. The

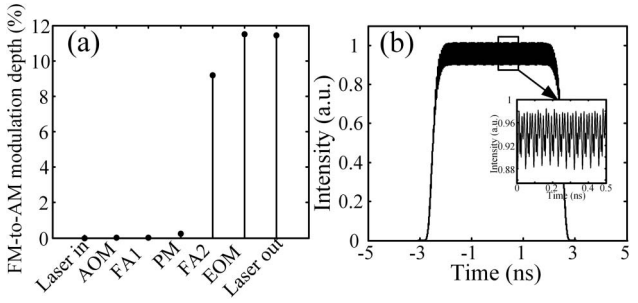

Fig. 5. FM-to-AM modulation in the PM fiber front-end. (a) FM-to-AM modulation distribution at different positions and (b) laser pulse with FM-to-AM modulation.

FM-to-AM modulation of the laser from the PM front end is 11.5%, as shown in Fig. 5(b), which is far larger than that from the PZ front end. The FM-to-AM modulation distribution in the PM system is also shown in Fig. 5(a), which indicates that the FM-to-AM modulation increases considerably after the second fiber amplifier and after the EOM. The FM-to-AM modulation shows no regularity and the main cause of the modulation is the PMD, so that the second order dispersion compensation has negligible effect on the laser pulse in the simulation. It should also be noted that the period of FM-to-AM modulation in the PM fiber front end is smaller than that of phase modulation frequency due to the interference of lasers along the slow and fast axis of the PM fiber, compared with the zoom-in of the FM-to-AM modulation of the PZ fiber front end in Fig. 3(b). Because of the polarization mode dispersion, the lasers along the slow and fast axis of PM fiber experience different delays and the coupling of the two orthogonal laser due to the low PERs of fiber elements and mode-coupling in the PM fiber induces the temporal interference, which can generate high order harmonic modulation. Different from the PM front end, the PZ fiber front end can eliminate the influence of the laser interference by a large loss of the fast axis, which is also another advantage over the PM front end. It should also be mentioned that the random phase shift φ_p has not been included in the aforementioned simulations. However, the FM-to-AM modulation theoretically fluctuates randomly in a large range owing to the random phase shift. To study the stability of the FM-to-AM conversion, the simulation is repeated 500 times for both PM fiber and PZ fiber front ends with the random phase in the range of zero to 2π and normal distribution of every PERs of the components in the front end, and the results are shown in Fig. 6 where the frequency represents the number of counts with certain FM-to-AM modulation depth.

The FM-to-AM modulation in the polarizing fiber system is quite stable compared with that of the PM fiber front end, where the FM-to-AM conversion fluctuates from 7% to over 70%. In the simulation, the PM fiber front end has the same structure with the polarizing fiber front end and no fiber polarizing element exists in the PM fiber front end. In reality, the PM fiber front end must have several fiber polarizing components to compensate for the depolarization caused by the mixing of two orthogonal polarization modes in the PM fiber, which can minimize the FM-to-AM modulation by increasing the polarization extinction ratio of the laser. However, the FM-to-AM modulation depth is still above 10% and fluctuates in a range over 20%, even if enough fiber polarizing components are inserted into the system. Additionally, the FM-to-AM modulation is mainly induced by the PMD, which makes the compensation extremely difficult compared with that of the PZ fiber front end, where the second-order dispersion is the predominant cause of FM-to-AM conversion. The PZ fiber is actually a PM fiber together with the distributed polarizing effect, so that the coupling between the fast axis and the slow axis is eliminated, which is the main cause of the FM-to-AM modulation for the PM fiber.

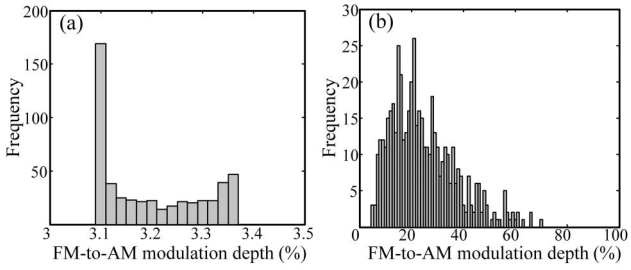

Fig. 6. Stability of FM-to-AM modulation depth. (a) In polarizing fiber front end, (b) in polarization-maintaining fiber front end.

As previously shown, the polarizing fiber front end has a great advantage over the PM fiber front end for the suppression of the FM-to-AM modulation. The modulation depth remains at a low level, which is mainly caused by second-order dispersion, and the stability of the FM-to-AM modulation is greatly improved so that the modulation fluctuates in a small range in the PZ fiber structure. The results indicate that a better performance can be obtained in the polarizing fiber front end. To verify simulation results, a front end made of polarizing fiber is constructed, and the experimental results are shown below.

4. EXPERIMENTAL RESULTS OF POLARIZING FRONT END SYSTEM

The structure of the polarizing fiber or the polarization maintaining fiber front end is shown in Fig. 7, where an arbitrary waveform generator (AWG) with a sampling rate of 25 Gb/s is used to shape the temporal profiles. Polarizing fiber (Fibercore, HB1060Z) is used as the PZ fiber whose polarizing effect is more than 30 dB for 5 m. In the experiment, the PM fiber and the PZ fiber front end have the same structure to compare the performance of FM-to-AM modulation. All of the components are made of PZ fiber in the PZ fiber front end except the DFB laser and the PM Yb-doped gain fiber. The PM fiber front end is only consisted of PM fiber patches and PM fiber components. Because the FM-to-AM modulation in the polarizing fiber front end is so small that it is difficult to accurately characterize the modulation depth, the phase-locking part, which can generate suitable electric modulation signals for the phase modulator, provides an external clock for the AWG so that the phase-modulation signal is phase locked with the electric signal for temporal shaping from the AWG. Through the phase-locking part, the FM-to-AM modulation is stable so that the modulation depth can be successfully characterized by the average process, which can eliminate the influence of noise. Considering the requirements of SBS and SSD, the laser spectrum is broadened with two modulation signals, 22 and 3 GHz,

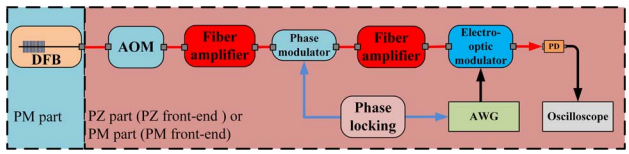

Fig. 7. Schematic of the polarizing fiber or polarization maintaining fiber front end. (DFB, distributed feedback laser; AOM, acoustic-optic modulator; AWG, arbitrary waveform generator; PD, high speed photodetector.)

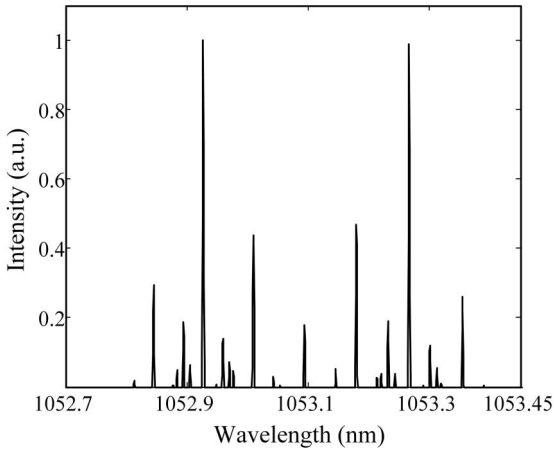

Fig. 8. Spectrum of laser from the polarizing fiber front end.

to over 0.3 nm. The spectrum of the laser is measured using a homemade spectrometer whose resolution is 5 pm, and Fig. 8 shows the detailed spectrum, where the sideband of 22 GHz is quite obvious and dominant. Compared with the situation of 22 GHz, the 3 GHz modulation signal is slightly weak but can still generate enough sidebands of 3 GHz, as shown in Fig. 8.

The actual polarizing fiber front end has the same structure as in the simulation, so that the experimental results can be directly compared with the simulation results. To accurately measure the FM-to-AM modulation of the front end, a high-speed oscilloscope with a 30 GHz bandwidth (Agilent, DSO93004L), together with a high-speed photodetector with a bandwidth of over 40 GHz (Newport, 1014), is implemented due to the short 50 ps period of the FM-to-AM modulation. The measured temporal profiles with the FM-to-AM modulation are shown in Fig. 9. Before the PZ fiber front end was built, a PM fiber front end, which had the same structure as the PZ fiber system, was studied. Figure 9(a) shows the temporal profile of the PM fiber front end, and the FM-to-AM modulation depth is over 20%. It should also be mentioned that the FM-to-AM modulation in the PM fiber system is quite unstable. The temporal profile in Fig. 9(a) is the typical case, and the FM-to-AM modulation in the PM system can fluctuate between several percent to nearly 20% during several minutes. Even under stable environmental conditions, the FM-to-AM modulation still fluctuates over a large range. This phenomenon is coincident with the simulation results and indicates that the PM fiber front end is not suitable to be used in the high-power laser facility, which demands a high, stable output.

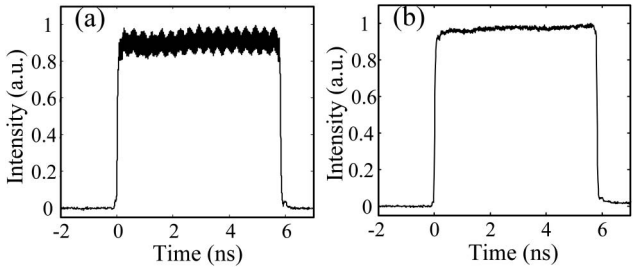

Fig. 9. Temporal profiles with FM-to-AM modulation. (a) In PM fiber front end, (b) in polarizing fiber front end.

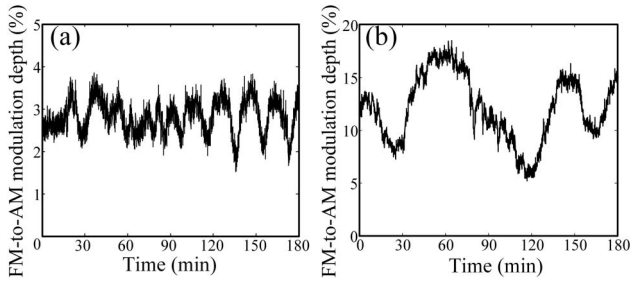

Fig. 10. Stability of FM-to-AM modulation depth during 3 h. (a) FM-to-AM modulation in the PZ fiber front end and (b) FM-to-AM modulation in the PM fiber front-end.

To overcome this obstacle, all the components in the front end are replaced with polarizing fiber components, as shown in Fig. 7, and the output temporal profile is compared with the PM fiber situation in Fig. 9(b). The modulation depth is less than 3%, which can hardly be observed. The FM-to-AM modulation is characterized at different positions in the front end, and it is found that the second polarizing fiber amplifier induces the largest FM-to-AM modulation, which is nearly 2%. Considering the analysis in the simulation part, this result is reasonable because of the relatively long fiber length in the amplifier. This phenomenon indicates that the GVD is the dominating cause of the FM-to-AM modulation in the polarizing fiber front end. To further suppress the modulation, a GVD compensation technique, which may involve a pair of gratings, can be implemented.

Another issue is the stability of the FM-to-AM modulation in the polarizing fiber front end. According to the simulation analysis, the FM-to-AM modulation fluctuates in a small range for the polarizing fiber front end. To characterize the stability of the modulation, the temporal profiles from the PZ fiber and PM fiber front end are monitored by an oscilloscope in real time for nearly 3 h, and the modulation depth is shown in Figs. 10(a) and 10(b). During those 3 h, the FM-to-AM modulation depth varies between 2% and 4% and the standard deviation (SD) of the modulation depth is 0.38%, whereas the FM-to-AM modulation depth of the PM fiber front end fluctuates over a range between 5% and 18% which is shown in Fig. 10(b). The fluctuation of the modulation depth indicates that the FM-to-AM modulation is quite stable, which is coincident with the simulation result.

Compared with the PM fiber front end, the polarizing fiber can successfully suppress the FM-to-AM modulation, which can be less than 3%, and the stability of the polarizing fiber is far better than that of the PM fiber. The experimental results verify the simulation results and prove that the polarizing fiber front end has a great advantage over the PM fiber front end. This result provides a promising structure to obtain a stable front end which can suppress the FM-to-AM modulation and improve the performance of the traditional front end in the high-power lasers such as ICF.

5. CONCLUSION

The evolution of FM-to-AM modulation in the complex front end is studied, and a model that can simulate the FM-to-AM

modulation both in polarization-maintaining fiber and polarizing fiber front end systems is established. In the simulation, the performance of the polarizing fiber is compared with that of the PM fiber under the structure of a real front end. The polarizing fiber structure can successfully suppress the FM-to-AM conversion and the analysis indicates that the GVD becomes the predominant factor in the polarizing fiber system, which can be easily compensated for with a pair of gratings. In addition to the aforementioned advantages, the FM-to-AM modulation is stable in the polarizing fiber structure, which is nearly impossible for the PM fiber case. The polarizing fiber front end is constructed for the first time to experimentally verify the simulation. According to the experimental results, the FM-to-AM modulation depth is suppressed to less than 3%, whereas the FM-to-AM modulation depth of the PM fiber front end is over 20%. The stability of the FM-to-AM modulation depth is 2% (peak–peak) and 0.38% (SD) over 3 h, which proves that the polarizing fiber front end is quite stable compared with the PM fiber system. Combining the simulation and experimental results, it can be concluded that the polarizing fiber front end has a great advantage over the PM fiber case. The polarizing fiber front end promises an excellent alternative to obtain better performance in the suppression of FM-to-AM modulation for high-power laser facilities, especially for laser ignition confinement fusion facilities.

Funding. National Natural Science Foundation of China (NSFC) (61205103, 61405211).

REFERENCES

1. C. A. Haynam, P. J. Wegner, and J. M. Auerbach, "National ignition facility laser performance status," Appl. Opt. **46**, 3276–3303 (2007).
2. M. L. Spaeth, K. R. Manes, M. Bowers, P. Celliers, J.-M. Di Nicola, P. Di Nicola, S. Dixit, G. Erbert, J. Heebner, D. Kalantar, O. Landen, B. MacGowan, B. Van Wonterghem, P. Wegner, C. Widmayer, and S. Yang, "National ignition facility laser system performance," Fusion Sci. Technol. **69**, 366–394 (2016).
3. V. Supradeepa, "Stimulated Brillouin scattering thresholds in optical fibers for lasers linewidth broadened with noise," Opt. Express **21**, 4677–4687 (2013).
4. J. R. Murray, J. R. Smith, R. B. Ehrlich, D. T. Kyrazis, C. E. Thompson, T. L. Weiland, and R. B. Wilcox, "Experimental observation and suppression of transverse stimulated Brillouin scattering in large optical components," J. Opt. Soc. Am. B **6**, 2402–2411 (1989).
5. S. Weber and C. Riconda, "Temperature dependence of parametric instabilities in the context of the shock-ignition approach to inertial confinement fusion," High Power Laser Sci. Eng. **3**, e6 (2015).
6. D. F. Browning, J. E. Rothenberg, and R. B. Wilcox, *The Issue of FM to AM Conversion on the National Ignition Facility* (Lawrence Livermore National Laboratory (LLNL), 1998).
7. C. Dorrer, "Spectral and temporal properties of optical signals with multiple sinusoidal phase modulations," Appl. Opt. **53**, 1007–1019 (2014).
8. C. Dorrer, R. Roides, R. Cuffney, A. V. Okishev, W. A. Bittle, G. Balonek, A. Consentino, E. Hill, and J. D. Zuegel, "Fiber front end with multiple phase modulations and high-bandwidth pulse shaping for high-energy laser-beam smoothing," IEEE J. Sel. Top. Quantum Electron. **19**, 219–230 (2013).
9. M. Temporal, B. Canaud, W. J. Garbett, R. Ramis, and S. Weber, "Irradiation uniformity at the Laser MegaJoule facility in the context of the shock ignition scheme," High Power Laser Sci. Eng. **2**, e8 (2014).
10. S. Vidal, J. Luce, and D. Penninckx, "Experimental demonstration of linear precompensation of a nonlinear transfer function due to second-harmonic generation," Opt. Lett. **36**, 88–90 (2011).
11. S. Hocquet, G. Lacroix, and D. Penninckx, "Compensation of frequency modulation to amplitude modulation conversion in frequency conversion systems," Appl. Opt. **48**, 2515–2521 (2009).
12. S. Hocquet, D. Penninckx, E. Bordenave, C. Gouédard, and Y. Jaouën, "FM-to-AM conversion in high-power lasers," Appl. Opt. **47**, 3338–3349 (2008).
13. D. Penninckx, N. Beck, J.-F. Gleyze, and L. Videau, "Signal propagation over polarization-maintaining fibers: problem and solutions," J. Lightwave Technol. **24**, 4197–4207 (2006).
14. J. R. Simpson, R. H. Stolen, F. M. Sears, W. Pleibel, J. B. Macchesney, and R. E. Howard, "A single-polarization fiber," J. Lightwave Technol. **1**, 370–374 (1983).
15. D. Nolan, G. Berkey, M.-J. Li, X. Chen, W. Wood, and L. Zenteno, "Single-polarization fiber with a high extinction ratio," Opt. Lett. **29**, 1855–1857 (2004).
16. D. Penninckx and N. Beck, "Definition, meaning, and measurement of the polarization extinction ratio of fiber-based devices," Appl. Opt. **44**, 7773–7779 (2005).
17. Z. Qiao, X. Wang, W. Fan, and Z. Lin, "Demonstration of a high-energy, narrow-bandwidth, and temporally shaped fiber regenerative amplifier," Opt. Lett. **40**, 4214–4217 (2015).

141.223.16.144 {ts '2017-02-25 18:24:56'}